





# Mechanical and Electrical Properties for ITO (Thin Film) Coating PET

Almo'men Bellah Alawnah <sup>1,\*</sup> , Ahed J Alkhatib <sup>2</sup> , Areej AlZoubi <sup>3</sup> , and Ola Hayajnah <sup>4</sup> 

<sup>1</sup> Industrial Engineering Department, Jordan University of Science and Technology;  
akalawnah19@eng.just.edu.jo

<sup>2</sup> Legal Medicine, Toxicology of Forensic Science and Toxicology Department, Jordan University of Science and Technology; ajalkhatib@just.edu.jo

<sup>3</sup> Computer Information Systems Department, Jordan University of Science and Technology;  
azalzoubi19@cit.just.edu.jo

<sup>4</sup> Computer Information Systems Department, Jordan University of Science and Technology;  
hayajnahola@gmail.com.

\* Correspondence: akalawnah19@eng.just.edu.jo

**Abstract:** This study focuses on applying ITO (Indium Tin Oxide) thin film as a PET (Polyethylene Terephthalate) coating in solar cells. While ITO thin films are already used in this field, their efficiency varies based on numerous factors, with the mechanical and electrical properties being the most influential. Understanding and optimizing these properties can significantly enhance the solar cell industry. To achieve this, we conducted film transmittance tests on the as-produced samples under various environmental conditions to investigate their material behavior. Additionally, mechanical and electrical experiments were carried out to analyze and compare these properties under different parameters, with the ultimate goal of improving the PET coating for solar cell applications. By studying and enhancing the performance of ITO thin films, we can contribute to advancements in solar cell technology.

**Keywords:** Indium Tin Oxide; Polyethylene Terephthalate Coating; Solar Cell.

---

## 1. Introduction

Indium tin oxide (ITO) is a transparent conducting material widely employed in numerous optoelectronic applications due to its excellent combination of high electrical conductivity and optical transparency [1, 2] while maintaining optical transparency [3]. Despite its well-established utility in various optoelectronic devices, the mechanical properties of ITO remain a crucial yet relatively unexplored aspect of its overall performance and reliability [4]. Understanding the mechanical properties, including hardness, adhesion, and flexibility, plays a pivotal role in optimizing the performance and reliability of ITO in practical applications [5]. Nevertheless, the mechanical properties of ITO play a vital role in determining its overall performance and reliability in real-world applications. Consequently, several studies have been conducted to delve into these mechanical properties, encompassing aspects such as hardness, adhesion, and flexibility. The success of ITO in these applications has largely focused on its electrical and optical characteristics, overlooking the crucial role of mechanical properties in ensuring long-term performance and reliability [6]. This paper addresses this knowledge gap by conducting an in-depth exploration of the mechanical attributes of ITO thin films. In this study, we specifically explored the mechanical properties of ITO films that were deposited on flexible substrates using a radio-frequency magnetron sputtering process. By

understanding and analyzing these mechanical characteristics, we aim to gain valuable insights that can further enhance the practical application of ITO films in optoelectronic devices.

## 2. Related Work

The study found that the hardness of the ITO films increased with the film thickness, while the adhesion between the ITO film and the substrate was influenced by the sputtering power and the annealing temperature. Additionally, the study revealed that the flexibility of the ITO films decreased with increasing film thickness, which could affect their performance in flexible electronics [7].

It investigated the effect of oxygen partial pressure during the sputtering deposition process on the electrical properties of ITO films. The study found that increasing the oxygen partial pressure led to an increase in the electrical resistivity and a decrease in the carrier concentration of the ITO films. Additionally, the study revealed that the mobility of the carriers in the ITO films decreased with increasing oxygen partial pressure, which could affect the overall electrical performance of ITO-based devices [8] also it investigated the optical properties of ITO films deposited by a sol-gel process. The study found that the optical transmittance of the ITO films in the visible range was influenced by the annealing temperature and the ITO film thickness.

The study also revealed that the reflectance of the ITO films increased with increasing film thickness, which could affect their performance in optoelectronic devices [9]. It investigated the influence of surface roughness on the optical properties of ITO films deposited by a magnetron sputtering process.

The study found that increasing the surface roughness of the ITO films led to an increase in their optical scattering, which could affect their transparency and optical performance. Additionally, the study revealed that the surface roughness of the ITO films was influenced by the deposition parameters such as sputtering power and substrate temperature [10]. It investigated the electrical and optical properties of ITO nanowires synthesized by a hydrothermal method.

The study found that the electrical conductivity of the ITO nanowires increased with increasing nanowire diameter, while their optical transmittance decreased. The study also revealed that the carrier concentration and mobility of the ITO nanowires were influenced by their nanostructured morphology, which could affect their overall performance in electronic and optoelectronic devices [11]. A study investigated the effects of Al doping on the electrical and optical properties of ITO films.

The study found that Al doping increased the electrical conductivity of the ITO films due to the formation of oxygen vacancies, which enhanced the carrier concentration and mobility. However, the study also revealed that excessive Al doping could result in a decrease in the optical transmittance of the ITO films, which could limit their transparency for certain applications [12]. A study investigated the mechanical and electrical properties of ITO thin films on flexible substrates.

The study found that the mechanical flexibility of ITO thin films was influenced by the film thickness, substrate curvature, and annealing temperature. The study also revealed that the electrical properties of the ITO thin films, including electrical conductivity and transparency, were maintained even under bending conditions, making them suitable for flexible electronics applications [13].

A study investigated the influence of post-deposition annealing on the electrical and optical properties of ITO films for solar cells. The study found that annealing at specific temperatures and durations could significantly affect the carrier concentration, mobility, and optical transmittance of

the ITO films, leading to improved performance in solar cell devices. The study also highlighted the importance of optimizing the annealing conditions to achieve the desired properties of ITO films for specific optoelectronic applications [14].

### 3. Devices and Methodology

We use many devices to complete our project, and we used the parts that we cut it from the sheet of (ITO) then we used the results that we got from these devices to analysis it by Minitab software.

#### Devices and Their Parts

- **Bending Fatigue Device (BFD)**

Bending fatigue of flexible solar cells is the most common failure mechanism that leads to crack the conductive thin film and ultimately fails the module. This bending can be happened on the flexible solar module during the manufacturing (see Figure 1). Furthermore, during the usage of the flexible solar module after production, it is bent around the surface that the device laid on. The bending during the usage is considered repetitive because the module is portable, in other word, it is laid around different surfaces during each time of relocate the module.

ITO and aluminum thin films were selected as an example on TCO and metallic thin films respectively. The flexible substrate was selected to be PET.

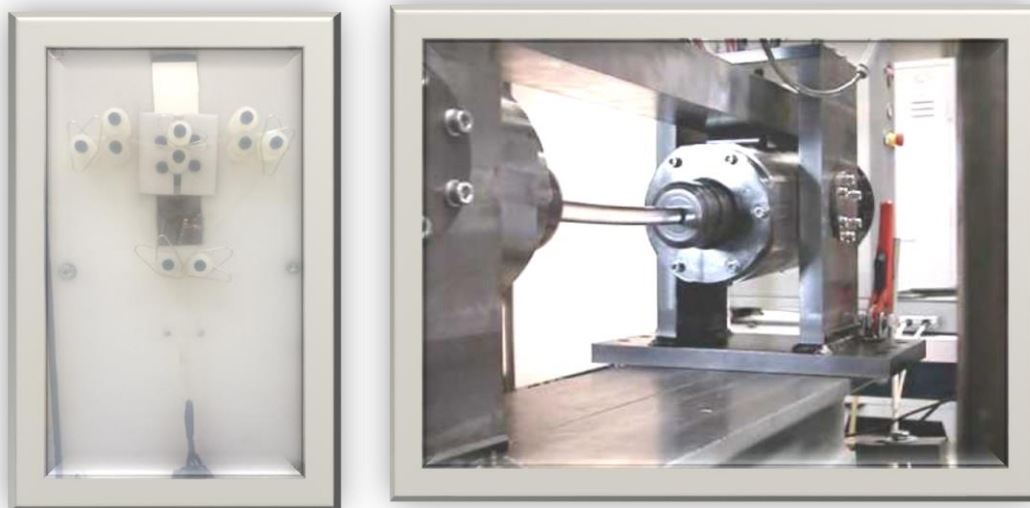


**Figure 1.** Bending Fatigue Device used in manufacturing laboratory, the right-hand side is similar to it.

The process of fatigue consists of three stages:

1. Initial fatigue damage leading to crack nucleation and crack initiation.
2. Progressive cyclic growth of a crack (crack propagation) until the remaining uncracked cross section of a part becomes too weak to sustain the loads imposed
3. Final, sudden fracture of the remaining cross section.

- **Shimadzu ag is 500 N (Universal Testing Machine)**

Is used to test the tensile strength and compressive and compressive strength of materials. An earlier name for a tensile testing machine is a tensometer. The "universal" part of the name reflects that it can perform many standard tensile and compression tests on materials, components, and structures (in other words that it is versatile, see Figure 2).



Figure 2. Shimadzu ag is 500 N.

- **Optical Microscope**

The optical microscope (see Figure 3), often referred to as the light microscope, is a type of microscope that uses visible light and a system of lenses to magnify images of small subjects. Optical microscopes are the oldest design of microscope and were possibly invented in their present compound form in the 17th century. Basic optical microscopes can be very simple, although many complex designs aim to improve resolution and sample contrast.



Figure 3. Optical microscope.

- **Ultra Volt spectrometer (See Figure 4)**



Figure 4. UV spectrometer.

#### Software's

- **LabVIEW**

Laboratory Virtual Instrument Engineering Workbench (LabVIEW) is a system-design platform and development environment for a visual programming language from National Instruments (see Figure 5).



Figure 5. LabVIEW logo.

- **Minitab**

Minitab is a statistics package developed at the Pennsylvania State University by researchers Barbara F. Ryan, Thomas A. Ryan, Jr., and Brian L. Joiner in 1972. It began as a light version of OMNITAB, a statistical analysis program by NIST; the documentation for OMNITAB was last published 1986, and there has been no significant development since then. Minitab is distributed by Minitab, Inc., a privately owned company headquartered in State College, Pennsylvania (see Figure 6).



Figure 6. Minitab 17 logo.

#### 4. Design and results

##### Tensile test

In this work, sputtered ITO thin film on poly ethylene terephthalate (PET) substrate samples with a two different sheet resistances, 100 and 60  $\Omega$  per square, of sputtered ITO thin film on PET substrate were stretched up to 30% of their initial length. The sample was gripped from both sides using Instron before allowing the upper and the lower grips to move away from each other, as shown in Figure 7, causing an increase in the substrate's length and decrease in its thickness.

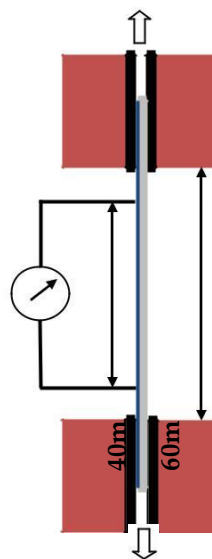


Figure 7. Schematic diagram of the specimen and grips.

Three different strain rates were considered to cover a wide range from very low, 0.01  $\text{min}^{-1}$  to very high, 1.0  $\text{min}^{-1}$  including a medium strain rate of 0.1  $\text{min}^{-1}$ . Under each strain rate, the electrical resistivity was measured after each 1% strain. Equations 1 and 2 refer to strain and strain rate respectively.

Where  $\Delta L$  is the increase of the sample length,  $L_o$  is the initial distance between grips, and  $T$  is the time in minutes. The initial length,  $L_o$ , was 60 mm which means 60 mm of the sample will be subjected to stretching. Also, the initial sample's thickness were 10 mm and 127  $\mu\text{m}$  respectively. In order to measure the electrical resistance during stretching, ohmmeter terminals were connected to the thin film at the location of 20 mm away from the grip. Therefore, the initial distance between the connection points was 40 mm (see Figure 8 and Figure 9).

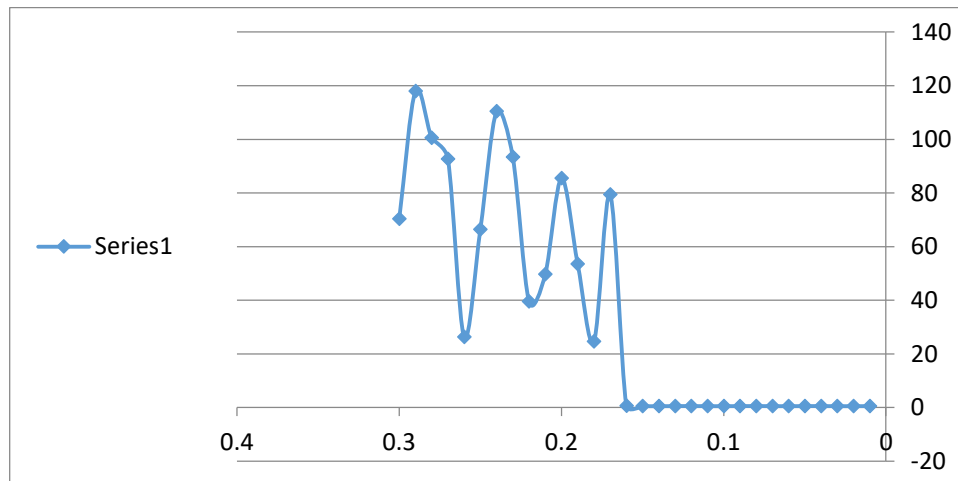


Figure 8. Relationship between Resistant and Strain for sample 100 and speed 60mm/min.

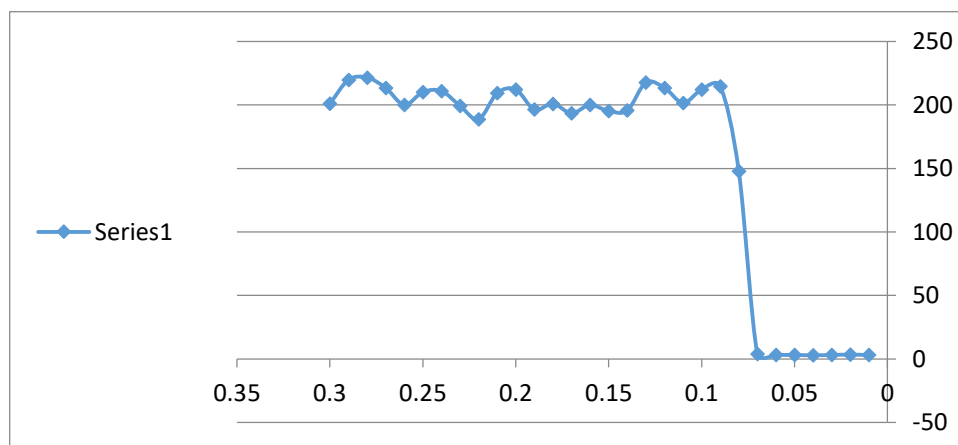


Figure 9. Relationship between Resistant and Strain for sample 300 and speed 180mm/min.

After collecting the electrical resistance readings, the relative electrical resistance change ( $R$ ) versus the strain was drawn at the different strain rates and sheet resistances. A comparison between the effects of strain rates on the  $R$  – strain curves were conducted for both sheet resistances. Optical microscope images were obtained after 60, 120, 180 speed to observe the formation and development



of cracks in each considered sheet resistance under different strain rates. The cracks intensity was captured and compared at these levels of strain and analyzed. DOE was used to investigate the effects of sheet resistance, strain rate, and strain on the crack intensity and the relative resistance change.

After getting the pieces we test it by the optical microscope we see these Figures 10- 17:



**Figure 10.** ITO 100 60\*10, **Figure 11.** ITO 100 120\*10



**Figure 12.** ITO 100 120\*100, **Figure 13:** ITO 100 180\*10

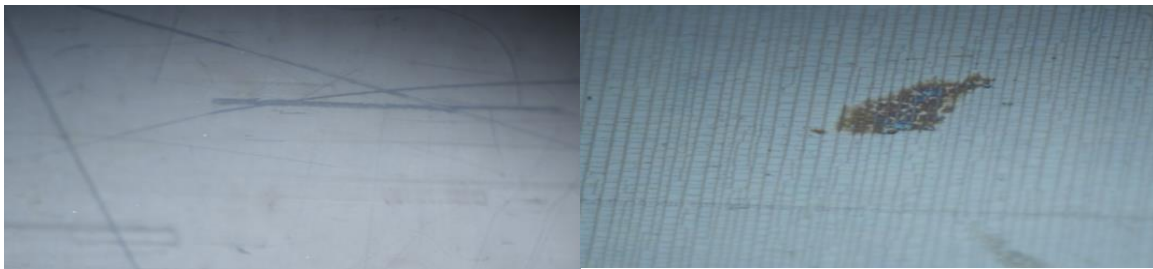


**Figure 14.** ITO 300 60\*10, **Figure 15.** ITO 300 60\*100



**Figure 16.** ITO 300 120\*10, **Figure 17:** ITO 300 180\*100



**Table 1.** ANOVA Table for the response *R*.

Source	DF		SS	MS	F	P
Sheet Resistance		1	3.38E+11	3.38019E+11	100.	0.000
Strain Rate		1	7.13 E+9	7135843690	2.13	0.155
Strain		1	4.8 E+10	4.8 E+10	14.3	0.001
Sheet Resistance× Strain Rate		1	2.66 E+9	2.66 E+9	0.79	0.380
Sheet Resistance× Strain		1	2.27 E+9	2.27 E+9	0.68	0.417
Strain Rate× Strain		1	3.15 E+9	3.15 E+9	0.94	0.340
Sheet Resistance×		1	2.8 E+9	2.81 E+9	0.84	0.367
Strain Rate× Strain						
Error		32	1.07E+11	3.36 E+9		
Total		39	5.1E+11			

$$S = 57938.2; R\text{-Sq} = 79.01\%; R\text{-Sq(aj)} = 74.41\%$$

Figure 18 shows the main effects of different factors on the relative electrical resistance change. The relative electrical resistance change was higher for the higher sheet resistance (thinner film) as can be seen in the Figure. Furthermore, the relative electrical resistance change was higher for the higher strain and strain rate. Although the higher level of strain rate was a hundred times of the lower level, it has the minimum effect on the response between the three considered factors. However, the sheet resistance had the maximum effect in this study. Figure 19 further shows the two factor interactions plot where no significant interaction between any two factors in term of affecting the relative electrical resistance change.

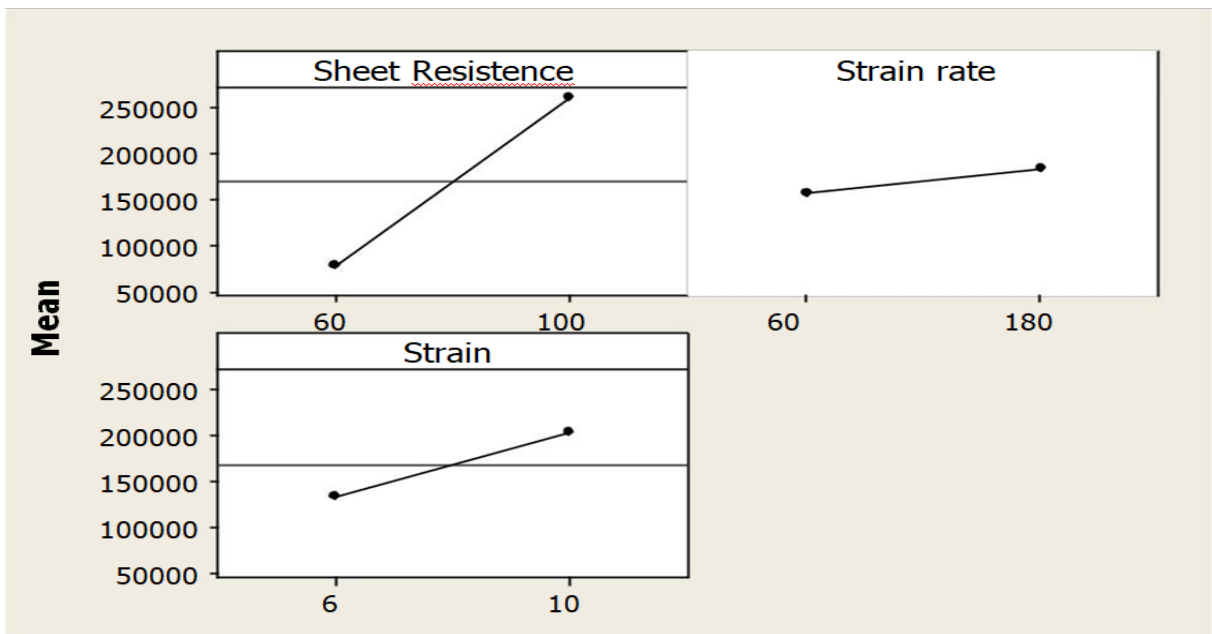


Figure 18. Main effect plot on the effect of sheet resistance, strain rate and strain on the relative electrical resistance change.

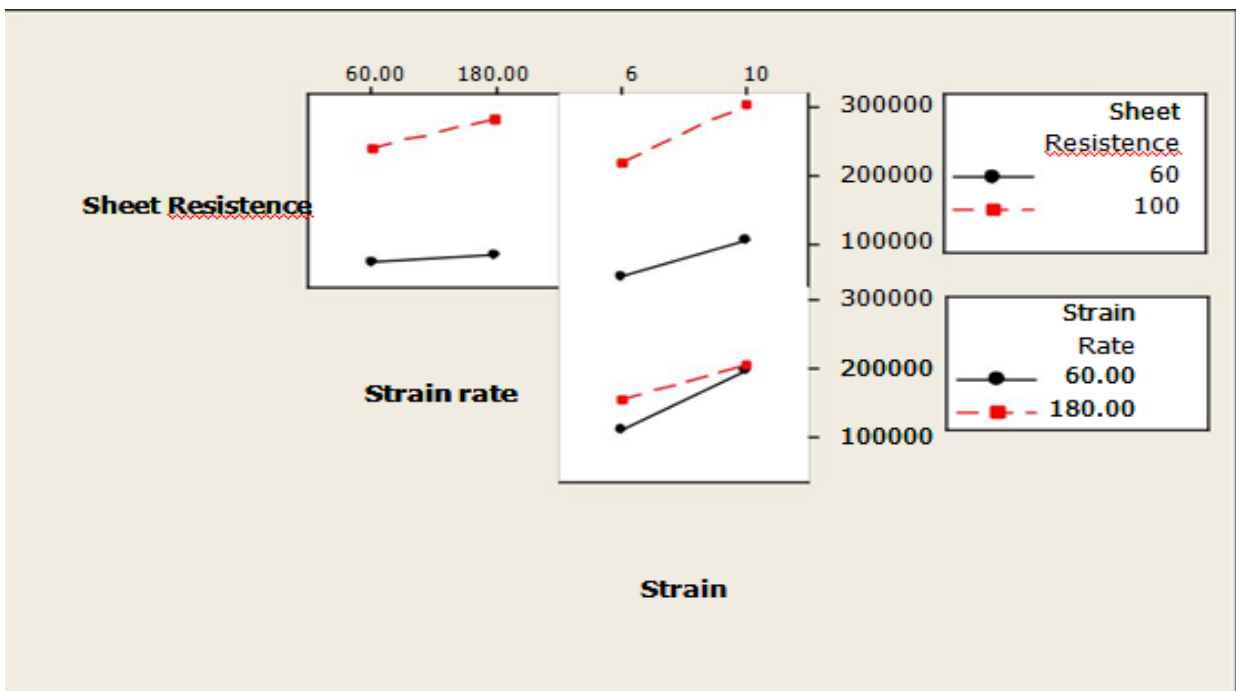


Figure 19. Two factor interactions plot on the effect of sheet resistance, strain rate and strain on the on the relative electrical resistance change.

*The UV test (transe)*

After getting the pieces from the tensile test we used to fix it and put it inside the device. The camera inside the device will give us the Trans calculated in excel and the drawing, here we will show the Tables 2- 5 that we got it and the Figures 20- 23.

- For ITO 100-clean

Table 2. ITO 100-clean.

Length wave	T%
252	0.06
253	0.063
254	0.06
255	0.051
256	0.023
257	0.031
258	0.048
259	0.065
260	0.049
261	0.02
262	0.038
263	0.042
264	0.049
265	0.054
266	0.038
267	0.029
268	0.045
269	0.042
270	0.05
271	0.027
272	0.013
273	0.03
274	0.023
275	0.038
276	0.051
277	0.037

- For ITO 100-60,120 and 180

Table 3: ITO 60,120 and 180.

	60	120	180
207	0.057	0.04	0.048
208	0.051	0.02	0.065
209	0.042	0.051	0.049
210	0.046	0.026	0.02
211	0.005	0.034	0.038
212	0.035	0.029	0.042
213	0.018	0.016	0.049
214	0.044	0.04	0.054
215	0.043	0.036	0.038
216	0.026	0.023	0.029
217	0.041	0.032	0.045
218	0.042	0.039	0.042
219	0.037	0.037	0.05
220	0.058	0.015	0.027
221	0.045	0.026	0.013
222	0.012	0.018	0.03
223	0.043	0.043	0.023
224	0.01	0.038	0.038
225	0.038	0.02	0.051
226	0.031	0.04	0.037
227	0.025	0.022	0.036
228	0.032	0.036	0.04
229	0.044	0.024	0.047
230	0.009	0.024	0.044
231	0.052	0.036	0.049

- For ITO 300 –clean

**Table 4.** ITO-clean.

<b>200</b>	<b>0.047</b>
<b>201</b>	0.04
<b>202</b>	0.048
<b>203</b>	0.044
<b>204</b>	0.023
<b>205</b>	0.037
<b>206</b>	0.038
<b>207</b>	0.032
<b>208</b>	0.022
<b>209</b>	0.031
<b>210</b>	0.021
<b>211</b>	0.024
<b>212</b>	0.03
<b>213</b>	0.039
<b>214</b>	0.04
<b>215</b>	0.029
<b>216</b>	0.02
<b>217</b>	0.039
<b>218</b>	0.034
<b>219</b>	0.032
<b>220</b>	0.032
<b>221</b>	0.027
<b>222</b>	0.027
<b>223</b>	0.043
<b>224</b>	0.032
<b>225</b>	0.024

- For ITO 300-60,120 and 180

Table 5: ITO 300 for 60,120 and 180.

	60	120	180
207	0.027	0.03	0.02
208	0.013	0.048	0.012
209	0.015	0.033	0.033
210	0.027	0.027	0.031
211	0.018	0.041	0.042
212	0.02	0.029	0.031
213	0.015	0.024	0.029
214	0.017	0.024	0.025
215	0.027	0.017	0.032
216	0.025	0.038	0.02
217	0.019	0.058	0.034
218	0.014	0.026	0.025
219	0.014	0.037	0.029
220	0.014	0.021	0.036
221	0.018	0.033	0.035
222	0.016	0.026	0.021
223	0.017	0.025	0.031
224	0.02	0.02	0.021
225	0.018	0.033	0.024
226	0.01	0.018	0.025
227	0.021	0.016	0.032
228	0.018	0.032	0.022
229	0.023	0.028	0.019
230	0.019	0.031	0.033
231	0.031	0.025	0.024



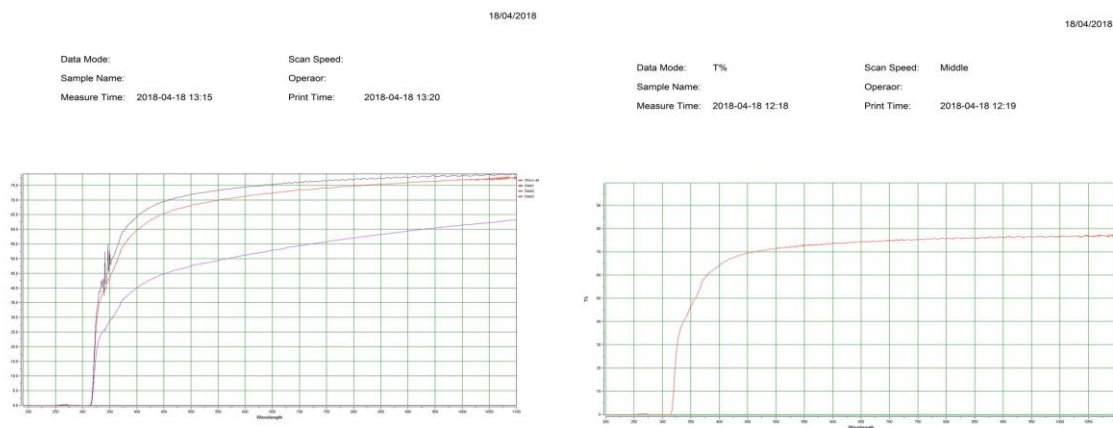


Figure 20. UV Test results (1). Figure 21. UV Test results (2).



Figure 22. UV Test results (3). Figure 23. UV Test results (4).

### The Bending test

The electrical resistance was measured using a two-point probe. A conductive copper tape was used to form terminals for the electrical resistance measurements to avoid direct contact between the probes and the surface of the thin film. Copper tape was used because it does not contribute to the thin film resistance. Alligator clips were used to make good contact between the copper tape and the ITO film. In each experiment, the change in electrical resistance was monitored at different time intervals during the test.

We use the parts ( $100 \Omega$  and  $60 \Omega$ ) for measure the resistance after the cycles. We use to but the part and the device do the fatigue test while it was fixed it by handles and measure the resistance by labVEIW. We tried to work by different types of parts, different speeds and different diameters (6mm and 14mm). And the number of cycle that we reach is 1500.

The result that we found that the resistance increase by increasing the number of cycle.

Results we got it (See Figures 24-27):

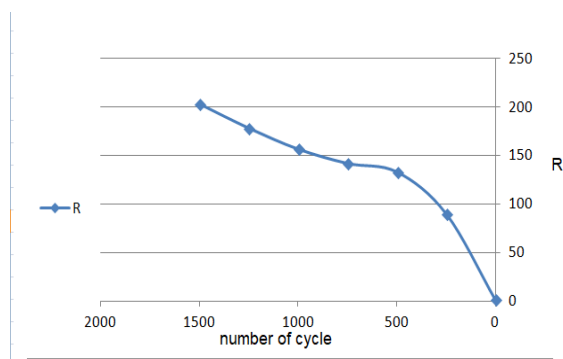
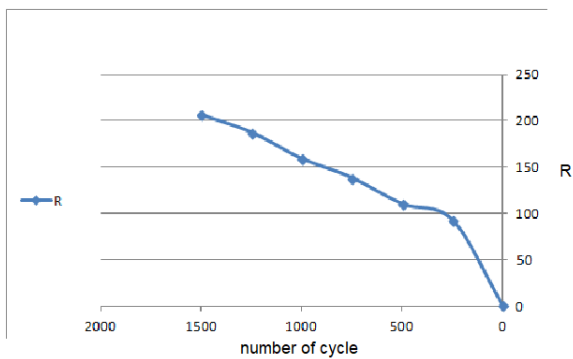


Figure 24: Bending fatigue test 60-high, 14 mm.

Figure 25: Bending fatigue test 60-high, 6 mm.

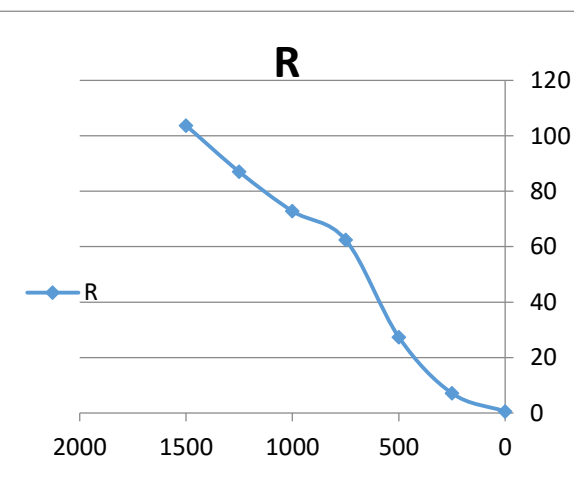
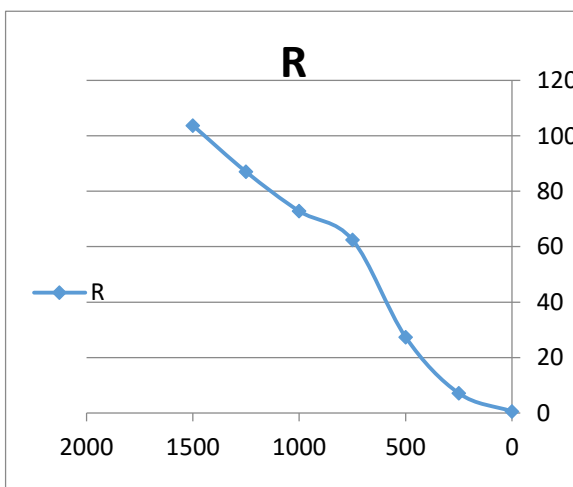


Figure 26: Bending fatigue test 100-low, 14 mm.

Figure 27: Bending fatigue test 100-high, 6 mm

### 5. Conclusions

This research delved into the impact of cyclic bending fatigue on indium tin oxide (ITO) thin films deposited on PET substrates. The high magnification optical microscopic examination revealed that the thin film's surface remained unchanged, indicating no visible signs of alteration. However, the behavior of the thin film was significantly affected by cyclic bending fatigue loadings. As the cycles of bending fatigue increased, the resistance of the thin film rose, and cracks were observed to initiate and propagate.

Of particular concern was the scenario involving cyclic bending fatigue loading combined with high temperature and high humidity conditions, which yielded the most adverse effects. To assess the thin film's performance under these conditions, electrical resistance measurements were conducted after every 30 cycles in a controlled chamber, equivalent to a total of 1500 cycles of cyclic bending. The results highlighted that the percent change in electrical resistance was most pronounced with a higher number of cycles under bending loads, corroborating the findings obtained from microscopic image analysis.

The outcomes of this study emphasize the critical significance of understanding the mechanical response of ITO thin films to cyclic bending fatigue, particularly in environments characterized by

elevated temperature and humidity. These findings are crucial for the development and design of robust optoelectronic devices, as they provide valuable insights into the material's behavior and potential weaknesses when subjected to cyclic stress.

Overall, this research contributes to the broader understanding of the performance and reliability of ITO thin films in real-world applications, particularly in flexible electronic devices. The knowledge gained from this investigation will aid in optimizing the design and manufacturing processes of such devices, with the ultimate aim of enhancing their durability and efficiency in diverse optoelectronic technologies. However, further studies may be warranted to explore additional aspects and refine the understanding of ITO thin film behavior under various stress conditions, paving the way for continued advancements in this rapidly evolving field.

### **Author Contributions**

All authors contributed equally to this work.

### **Funding**

This research was conducted without external funding support.

### **Ethical approval**

This article does not contain any studies with human participants or animals performed by any of the authors.

### **Conflicts of Interest**

The authors declare that there is no conflict of interest in the research.

### **Institutional Review Board Statement**

Not applicable.

### **Informed Consent Statement**

Not applicable.

### **Data Availability Statement**

Not applicable.

### **References**

- [1] Kim, J., Jo, G., & Lee, W. "Transparent conducting oxides: The past and future." *Journal of Materials Science*, 48(2), 249-270.
- [2] Liu, Y., Wei, H., & Wang, X. "Recent advances in indium tin oxide-based optoelectronic devices." *Advanced Materials*, 30(20), 1704385.
- [3] Chen, X., Liu, Y., & Yan, Z. "Transparent conductive oxide materials for optoelectronic applications." *Frontiers of Optoelectronics*, 13(3), 185-198.

- [4] Singh, S., Gupta, A., & Sharma, R. "Mechanical properties of indium tin oxide films: A review." *Surface & Coatings Technology*, 406, 126546.
- [5] Sahoo, S. K., Panda, S., & Panigrahi, S. "Mechanical characterization of ITO thin films on flexible substrates." *Journal of Materials Science: Materials in Electronics*, 29(10), 8275-8282.
- [6] Park, J., Kim, J., & Lee, J. "Mechanical properties of ITO thin films on flexible substrates." *Thin Solid Films*, 692, 137850.
- [7] Kim, D., Kim, M., Seo, H., Park, S., & Jung, S. (2017). Mechanical properties of indium tin oxide films deposited on flexible substrates by radio-frequency magnetron sputtering. *Journal of Vacuum Science & Technology A*, 35(6), 061503.
- [8] Sharma, A., Saxena, A., Tomar, M., & Dhawan, S. K. (2018). Effect of oxygen partial pressure on electrical properties of indium tin oxide thin films deposited by RF magnetron sputtering. *Journal of Materials Science: Materials in Electronics*, 29(8), 6698-6706.
- [9] Wu, L., Zhang, Q., Lin, X., Huang, X., Liu, Y., & Deng, Z. (2019). Influence of annealing temperature and film thickness on optical properties of ITO films deposited by sol-gel process. *Optics and Laser Technology*, 109, 285-290.
- [10] Liu, Z., Cheng, K., Chen, H., & Gao, S. (2016). Influence of surface roughness on the optical properties of ITO films prepared by magnetron sputtering. *Applied Surface Science*, 370, 499-505.
- [11] Wang, W., Ye, C., Zhang, X., & Zhou, T. (2018). Electrical and optical properties of ITO nanowires synthesized by hydrothermal method. *Materials Research Bulletin*, 105, 95-101.
- [12] Jeong, C., Kim, K., Kim, D., & Kim, J. (2019). Effects of Al doping on the electrical and optical properties of ITO films. *Journal of Materials Science*, 54(5), 4106-4115.
- [13] Guo, X., Zhang, Y., Liao, X., Xu, K., & Zhu, Z. (2017). Mechanical and electrical properties of indium tin oxide thin films on flexible substrates. *Thin Solid Films*, 635, 68-75.
- [14] Kim, J., Kim, J., Lee, H., & Cho, H. (2018). Effects of post-deposition annealing on the electrical and optical properties of indium tin oxide films for solar cells. *Journal of Materials Science: Materials in Electronics*, 29(13), 10817-10825

**Received:** 28 Oct 2023, **Revised:** 10 Feb 2024,

**Accepted:** 05 Mar 2024, **Available online:** 11 Mar 2024.



© 2024 by the authors. Submitted for possible open access publication under the terms and conditions of the Creative Commons Attribution (CC BY) license (<http://creativecommons.org/licenses/by/4.0/>).